Central European Journal of Energetic Materials
ISSN 1733-7178; e-ISSN 2353-1843

Cent. Eur. J. Energ. Mater., 2016, *13*(4), 871-881; DOI: 10.22211/cejem/63747

Preparation and Properties of RDX-Nitrocellulose Microspheres

Xiaofeng SHI,* Jingyu WANG, Xiaodong LI

Chemical Industry and Ecology Institute, North University of China, Shanxi, 030051 Taiyuan, P. R. China
**E-mail: xiaofeng_shi1987@163.com*

Abstract: A new insensitive explosive based on RDX and with Nitrocellulose (NC) as binder has been prepared using a flash vaporization process. Scanning electron microscopy was used to characterize the morphology and particle size of the resulting RDX-NC microspheres. X-ray photoelectron spectroscopy, Differential Scanning Calorimetry, impact sensitivity, vacuum stability and burning rate of raw RDX, RDX-NC and RDX-1 were also used to characterize the explosive. The RDX-NC microspheres were found to have a fibrous surface. The microspheres ranged in size from 0.5 μm to 4 μm. The NC formed a coat on the surface of the RDX. The activation energies of raw RDX, RDX-1 and RDX-NC were found to be 200.8 kJ·mol^{-1}, 183.9 kJ·mol^{-1} and 187.2 kJ·mol^{-1}, respectively. The drop heights of raw RDX, RDX-1 and RDX-NC were found to be 21.3 cm, 51.7 cm and 82.9 cm, respectively. The friction sensitivity of RDX-NC was lower than that of raw RDX and RDX-1. In the vacuum stability test, the volumes of evolved gas from raw RDX, RDX-1 and RDX-NC were 0.12 mL·g^{-1}, 0.12 mL·g^{-1}, and 0.09 mL·g^{-1}, respectively. The burning rates of RDX-NC-based propellants were higher than that of RDX-1 and raw RDX based propellants at 5-15 MPa. The burning rate pressure exponent of RDX-NC based propellants is 0.9929 at 40-200 MPa.

Keywords: RDX, nitrocellulose, flash vaporization process, thermal stability

Nomenclature List

H_{50} = 50% explosion probability,
S = standard deviation,
β_i = heating rate in K·min^{-1},
T_{pi} = the temperature of the exothermic peak at β_i heating rate in K,
E = the activation energy in J·mol^{-1},
A = the pre-exponential factor,
R = the gas constant, 8.314 J·mol^{-1}·K^{-1}.

1 Introduction

There is a growing requirement for the energy of composite modified double-base (CMDB) propellants to be increased [1, 2]. The most common approach to increase the energy of CMDBs is by the addition of nitramine explosives and RDX is the one commonly used to do this [3-6]. But adding RDX produces many problems, such as higher mechanical sensitivity and worse mechanical properties [7-10]. Previous research has shown that reducing the size of solid filler particles can solve these problems and also enhance the burning rate of propellants [11-14]. In addition, the mechanical sensitivity of CMDBs can be decreased if the particles coated with some binders [15-18]. Nitrocellulose (NC) is necessary for the energy and mechanical properties of double-base propellants. Using NC as a binder can avoid mixing unnecessary impurities into the propellants. Spheroidization is another way to solve the problem of high mechanical sensitivity [19-21].

In our previous study, we prepared a type of spherical HMX/NC nano-composites. NC was not coated onto the surface of the HMX. Instead, the HMX nano-particles and NC were found to combine well [22]. But the vacuum stability of that mix was not good. In the research reported in the present paper, we prepared pure RDX (labelled as RDX-1) and RDX-NC microspheres (labelled as RDX-NC) by a flash vaporization process. NC was coated onto the surface of the RDX. We then characterized and analyzed the sample properties in detail.

2 Experimental Section

2.1 Preparation of RDX-NC Microspheres

10 g of RDX (provided by the Gansu Ying Guang Chemical Industry Group Co., Ltd.), which particle size and morphology are shown in Figure 2a, and 0.5 g of NC (provided by the China North Chemical Industries Group Co., Ltd.) were dissolved at 35 °C in 200 g of acetone (purchased from the Tianjin TianDa Chemicals Co., Ltd.) to form a uniform co-solution by sonication. As is shown in Figure 1, nitrogen gas was heated using an electrical heater (labelled a). The heating temperature and flow rate of the nitrogen were set as 55 °C and 430 $L \cdot h^{-1}$, respectively. The RDX solution and hot nitrogen were then sprayed from a nozzle (labelled b) and dried to produce microspheres. The flow rate of the feed solution was set to 10 $mL \cdot min^{-1}$. When the hot nitrogen and solution had gone through a cyclone separator (labelled c), the dried particles were collected in an electrically grounded glass collection vessel (labelled d) and the

gas exhausted to a recovery system (labelled e).

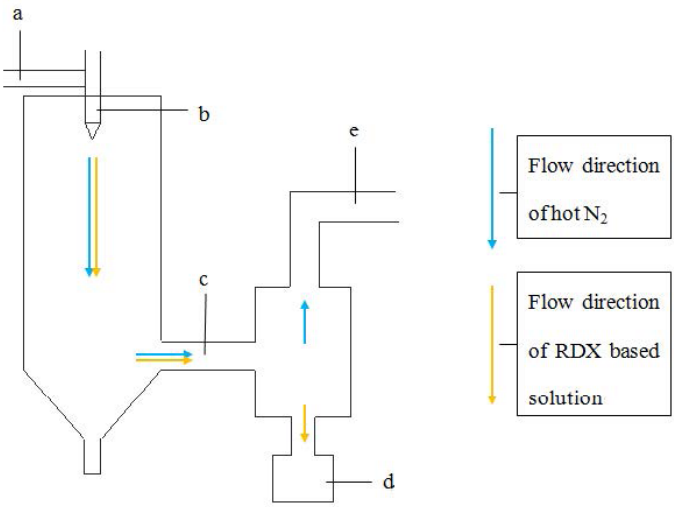

Figure 1. Flow chart of flash vaporization process set up.

2.2 Characterization

The size and morphology of the samples were surveyed using an S-4800 scanning electron microscope (SEM) (Hitachi Ltd., Japan). Axis Ultra Imaging Photoelectron Spectrometer (Kratos Analytical Ltd., England) was used to contrast the surface elements of the raw RDX, RDX-1 and RDX-NC nanocomposites by X-ray photoelectron spectroscopy (XPS). Differential scanning calorimetry (DSC) experiments were conducted in a N_2 atmosphere using a Setaram DSC131 instrument (Setaram instrumentation Co., France). The test conditions were: sample mass, 0.7 mg; N_2 flow rate, 15 mL·min^{-1} and sample heating rates, 20, 10 and 5 K·min^{-1}. The impact sensitivities of samples were determined at room temperature using an Explosive Research Laboratory (ERL) type 12 drop hammer apparatus with a sample mass of 35 ± 1 mg and a drop weight of 5 ± 0.002 kg. Two groups of each sample and 25 of the same samples from each group were tested. The results are reported in terms of the critical drop-height of 50% explosion probability (H_{50}) and the standard deviation (S). Vacuum Stability was tested by a Stabil 21 dynamic vacuum stability apparatus. Standard techniques were used to measure the burning rate. The initial temperature was 298 K.

3 Results and Discussion

3.1 Scanning Electron Microscope Characterization

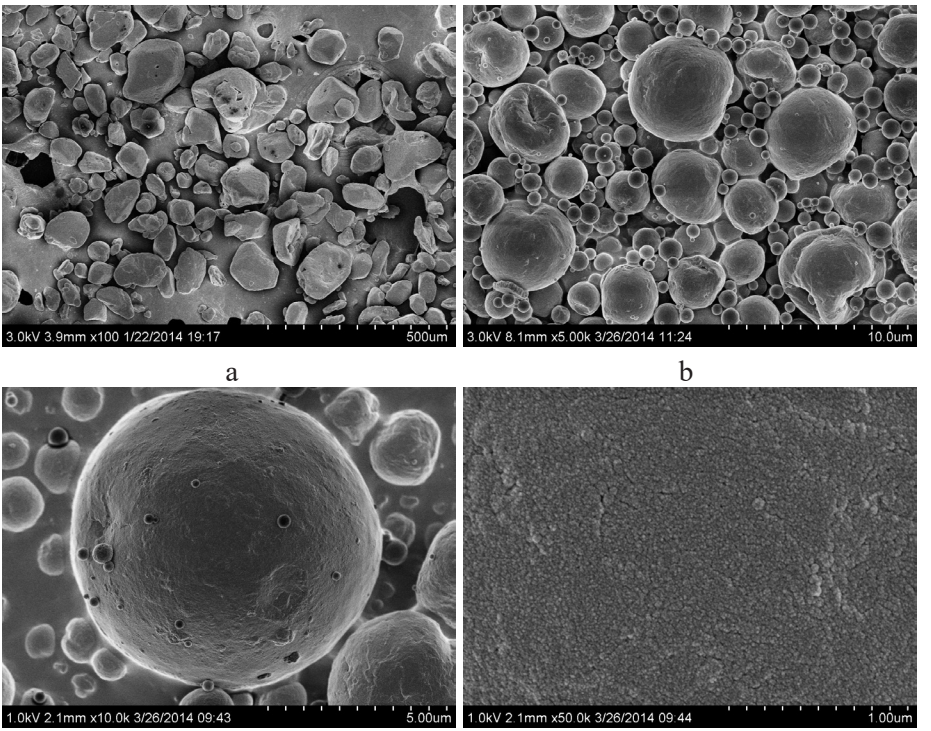

Figure 2. SEM images of (a) raw RDX and (b-d) RDX-NC microspheres at different magnifications.

Figure 2 shows SEM micrographs of raw RDX and RDX-NC microspheres. As is shown in Figure 2a, the raw RDX in the size range from 50 μm to 150 μm is blocky. Figure 2b shows that the particle size of RDX-NC ranges from 0.5 μm to 4 μm. The samples were microspherical, with a smooth (see Figure 2c) yet fibrous surface (see Figure 2d).

3.2 X-ray photoelectron spectroscopy characterization

The distribution of raw RDX and RDX-NC surface elements were characterized by XPS. The results are shown in Table 1.

Table 1. Distribution of raw RDX and RDX-NC surface elements

Samples	Surface elements [%]		
	O 1s	N 1s	C 1s
Raw RDX	36.07	39.80	24.13
RDX-NC	34.80	20.32	44.88

As is shown in Table 1, the "O" content of raw RDX and RDX-NC is similar. The "N" content of RDX-NC decreases sharply while the "C" content increases significantly compared with raw RDX. It can be explained that the "N" content of NC is less than that of raw RDX, and the "C" content of NC is greater than that of raw RDX. The original surface distribution of elements is changed when raw RDX is coated with NC.

3.3 Thermal decomposition characteristics

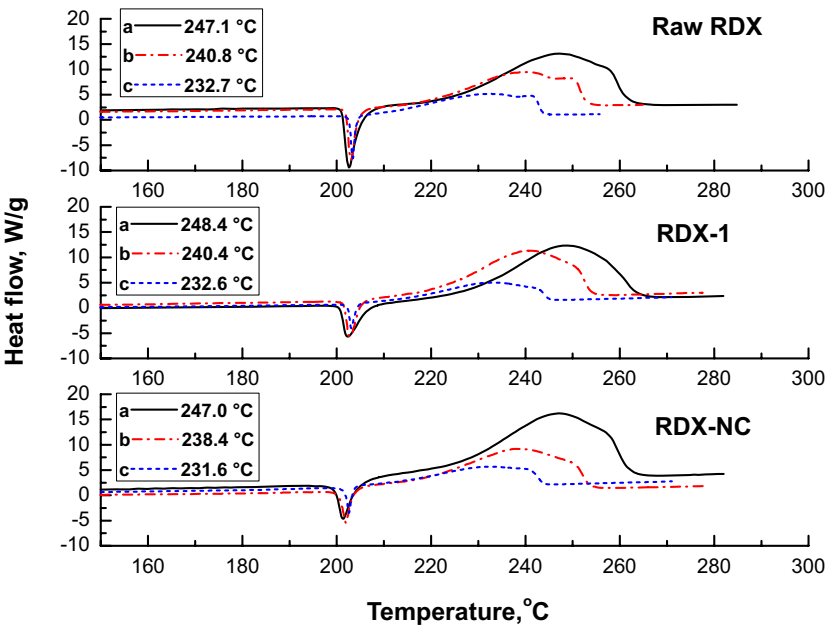

Figure 3. DSC curves of raw RDX, RDX-1 and RDX-NC at heating rates of (a) 20 K·min^{-1}, (b) 10 K·min^{-1}, and (c) 5 K·min^{-1}.

Figure 3 shows DSC curves of raw RDX, and RDX-1 and RDX-NC microspheres at 20 K·min^{-1}, 10 K·min^{-1} and 5 K·min^{-1} heating rates. There is an endothermic peak at 201~203 °C in all the DSC curves in Figure 3. These

curves show that the RDX began to melt at 201~203 °C. For the same sample, the exothermic peak temperatures are lower at slower heating rates. The thermal decomposition kinetics parameters of raw RDX, and the RDX-1 and RDX-NC microspheres can be calculated using the Kissinger method (Equation 1) [23].

$$\ln\frac{\beta_i}{T_{pi}^2} = \ln\frac{AR}{E} - \frac{E}{RT_{pi}} \tag{1}$$

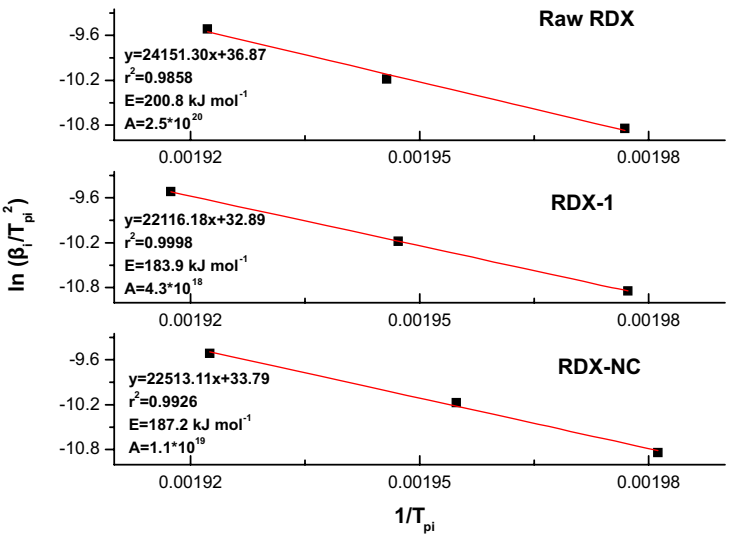

Figure 4. Kissinger's plot of raw RDX, RDX-1 and RDX-NC microspheres.

As is shown in Figure 4, a straight line is obtained when the values of $ln(\beta_i/T_{pi}^2)$ are plotted against $1/T_{pi}$. The activation energy can be calculated from the slope $(-E/R)$. The pre-exponential factor can be calculated from the intercept $[ln(AR/E)]$. The results show that the activation energies of raw RDX, RDX-1 and RDX-NC microspheres are 200.8 ± 17.0 kJ·mol^{-1}, 183.9 ± 0.5 kJ·mol^{-1} and 187.2 ± 11.4 kJ·mol^{-1}, respectively. Compared with raw RDX, the activation energies of RDX-1 and RDX-NC are lower by about 16.9 kJ·mol^{-1} and 13.6 kJ·mol^{-1}, respectively.

3.4 Impact sensitivity

From Table 2, it can be seen that the drop height of RDX-1 is higher than that of raw RDX (two repeat experiments were performed). The drop height of RDX-NC is much higher than that of raw RDX and RDX-1. These results prove that the

impact sensitivity of RDX-1 is lower than that of raw RDX and that the addition of NC can reduce the impact sensitivity of RDX. Our drop-height measurements compare favorably with those reported by Armstrong [24].

3.5 Vacuum stability test

Vacuum stabilities of samples were tested by keeping samples at 100 °C for 48 hours under vacuum.

Table 2. Impact sensitivity and vacuum stability of raw RDX, RDX-1 and RDX-NC

Samples	Impact sensitivity, H_{50} [cm]			Vacuum stability test
	Experiment 1 (*S*)	Experiment 2 (*S*)	Average	Volume of evolved gas [mL·g^{-1}]
Raw RDX	20.2 (0.06)	22.4 (0.03)	21.3	0.12
RDX-1	50.5 (0.02)	52.8 (0.05)	51.7	0.12
RDX-NC	80.3 (0.04)	85.4 (0.07)	82.9	0.09

The volume of gas released from 1.0 g samples is much less than 2.0 mL at 100 °C showing that the raw RDX, RDX-1 and RDX-NC are all relatively stable and safe during usage and storage according to the Standard of Vacuum Stability [25]. The gas volume evolved from RDX-NC is lower than that from raw RDX and RDX-1. This can be explained as due to the NC (which was coated onto the surface of RDX) partly eliminating the active decomposition reaction centers of RDX. Therefore, the thermal stability of RDX-NC is better than that of both raw RDX and RDX-1.

3.6 Friction sensitivity

Table 3. Friction sensitivities of raw RDX, RDX-1 and RDX-NC

Samples	Friction sensitivity [%]
Raw RDX	88
RDX-1	16
RDX-NC	9

As is shown in Table 3, the friction sensitivity of RDX-1 is lower than that of raw RDX. Also the friction sensitivity of RDX-NC is lower than that

of RDX-1 and raw RDX. This proves that the addition of NC can reduce the friction sensitivity of RDX.

3.7 Burning rate

In the burning rate tests, the formulation of RDX-CMDB propellants is: raw RDX/RDX-1/RDX-NC (30%); NC (32%); NG/DINA (36%); other materials (2%). The results are shown in Table 4.

Table 4. Burning rate of RDX-CMDB propellants at high pressure (pressure range: 5-15 MPa)

Samples	Fillers	Burning rate, u [mm·s^{-1}] at different pressures		
		5 MPa	10 MPa	15 MPa
1	Raw RDX	4.23	7.95	9.82
2	RDX-1	5.01	8.33	10.12
3	RDX-NC	5.29	8.48	10.20

Table 4 shows the effect of propellant composition on burning rate. The burning rate of samples 2 and 3 increased more over the pressure range 5~15 MPa compared with sample 1. The burning rate of sample 3 was faster than that of sample 2. This proves that RDX-1 and RDX-NC all can enhance the burning rate of RDX based propellants. This effect is more obvious for RDX-NC than for RDX-1.

The burning rate pressure exponent of RDX-NC based propellants was also studied. The result is shown in Table 5.

Table 5. Burning rate pressure exponent of RDX-NC based propellants at different pressure intervals

Sample	P [MPa]			
RDX/NC based propellants	40-80	80-120	120-200	40-200
	1.2313	1.1165	0.9712	0.9929

From Table 5, it can be seen that the burning rate pressure exponent of RDX-NC based propellants decreases as the pressure increases. This shows that the effect of pressure change on the burning rate will be small when the pressure is high.

4 Conclusions

An RDX-based microsphere, which was coated with NC, was prepared successfully by a flash vaporization process. The microspheres were 0.5 μm to 4 μm in size and the surfaces exhibited a fibrous shape. Pure RDX (RDX-1) was also prepared by the same process. The proportion of elements in the surface of RDX-NC was very different to that of raw RDX. This is because of the NC coating on the surface of RDX which changes the proportion of surface elements originally present. The activation energy of RDX-NC is lower than that of raw RDX but a little higher than that of RDX-1. The impact sensitivities of RDX-1 and RDX-NC were lower than that of the raw RDX because of a greater drop height. The friction sensitivity of RDX-NC was lower than that of raw RDX and RDX-1. The thermal stabilities of RDX-1 and raw RDX were basically similar. The thermal stability of RDX-NC was better than that of the other two samples. The burning rate of RDX-NC microspheres based propellants was higher than that of RDX-1 and raw RDX based propellants. The burning rate pressure exponent of RDX-NC based propellants is 0.9929 at 40-200 MPa. These combined properties suggest that RDX-NC microspheres are an insensitive spherical explosive with great potential in solid propellants.

References

[1] Jin B., Peng R.F., Zhao F.Q., Yi J.H., Xu S.Y., Wang S.B., Chu S.J., Combustion Effects of Nitrofulleropyrrolidine on RDX-CMDB Propellants, *Propellants Explos. Pyrotech.*, **2014**, *39*(6), 874-880.

[2] Hou Z.L., Feng Z.G., Wang E.P., Han P.M., The Energy and Pressure Exponent of Composite Modified Double-base Propellant, *Propellants Explos. Pyrotech.*, **1992**, *17*(2), 59-62.

[3] Divekar C.N., Asthana S.N., Singh H., Studies on Combustion of Metallized RDX-Based Composite Modified Double-Base Propellants, *J. Propul. Power*, **2001**, *17*(1), 58-64.

[4] Qin M.N., Zheng X.D., Yan Q.L., Yuan T.G., Tang W., Li H.L., Qiu S.J., Sol-gel Preparation of PZT Powders and Its Catalytic Effect on Burning Rate of RDX-CMDB Propellant, *Sci. Technol. Energ. Mater.*, **2012**, *73*(3-4), 88-92.

[5] Asthana S.N., Athawale B.K., Singh H., Impact, Friction, Shock Sensitivities and DDT Behaviour of Advanced CMDB Propellants, *Def. Sci. J.*, **2013**, *39*(1), 99-107.

[6] Raman K.V., Singh H., Ballistic Modification of RDX-Based CMDB Propellants, *Propellants Explos. Pyrotech.*, **1988**, *13*(5), 149-151.

[7] Li T., Hua C., Li Q., Shock Sensitivity of Pressed RDX-Based Plastic Bonded Explosives under Short-Duration and High-Pressure Impact Tests, *Propellants*

Explos. Pyrotech., **2013**, *38*(6), 770-774.
[8] Essel J.T., Cortopassi A.C., Kuo K.K., Leh Ch.G., Adair J.H., Formation and Characterization of Nano-sized RDX Particles Produced Using the RESS-AS Process, *Propellants Explos. Pyrotech.*, **2012**, *37*(6), 699-706.
[9] Swadley M.J., Li T.L., Reaction Mechanism of 1,3,5-Trinitro-s-triazine (RDX) Deciphered by Density Functional Theory, *J. Chem. Theory Comput.*, **2007**, *3*(2), 505-513.
[10] Ismael C.R., Zoltán T., Nan T., Chen H.W., Graham C.R., Desorption Electrospray Ionization of Explosives on Surfaces: Sensitivity and Selectivity Enhancement by Reactive Desorption Electrospray Ionization, *Anal. Chem.*, **2005**, *77*(21), 6755-6764.
[11] Hudson R.J., Zioupos P., Gill P.P., Investigating the Mechanical Properties of RDX Crystals Using Nano-Indentation, *Propellants Explos. Pyrotech.*, **2012**, *37*(2), 191-197.
[12] Liu J., Jiang W., Zeng J.B., Yang Q., Wang Y.J., Li F.S., Effect of Drying on Particle Size and Sensitivities of Nano Hexahydro-1,3,5-trinitro-1,3,5-triazine, *Def. Technol.*, **2014**, *10*(1), 9-16.
[13] Naya T., Kohga M., Influences of Particle Size and Content of HMX on Burning Characteristics of HMX-based Propellant, *Aerosp. Sci. Technol.*, **2013**, *27*(1), 209-215.
[14] Naya T., Kohga M., Influences of Particle Size and Content of RDX on Burning Characteristics of RDX-based Propellant, *Aerosp. Sci. Technol.*, **2014**, *32*(1), 26-34.
[15] Elbeih A., Jungová M., Zeman S., Vávra P., Akštein Z., Explosive Strength and Impact Sensitivity of Several PBXs Based on Attractive Cyclic Nitramines, *Propellants Explos. Pyrotech.*, **2012**, *37*(3), 329-334.
[16] Joseph M.D., Jangid S.K., Satpute R.S., Polke B.G., Nath T., Asthana S.N., Rao A.S., Studies on Advanced RDX/TATB Based Low Vulnerable Sheet Explosives with HTPB Binder, *Propellants Explos. Pyrotech*, **2009**, *34*(4), 326-330.
[17] Shi X.F., Wang J.Y., Li X.D., An C.W., Preparation and Characterization of HMX/Estane Nanocomposites, *Cent. Eur. J. Energ. Mater.*, **2014**, *11*(3), 433-442.
[18] Shi X.F., Wang J.Y., Li X.D., An C.W., Ji W., Wang J., Preparation and Properties of 1,3,5,7-Tetranitro-1,3,5,7-tetrazocane based Nanocomposites, *Def. Sci. J.*, **2015**, *65*(2), 131-134.
[19] Shi X.F., Wang C.L., Wang J.Y., Li X.D., An C.W., Ji W., Wang J., Process Optimization and Characterization of an HMX/Viton Nanocomposite, *Cent. Eur. J. Energ. Mater.*, **2015**, *12*(3), 487-495.
[20] Sivabalan R., Gore G.M., Nair U.R., Saikia A., Venugopalan S., Gandhe B.R., Study on Ultrasound Assisted Precipitation of CL-20 and Its Effect on Morphology and Sensitivity, *J. Hazard. Mater.*, **2007**, *139*(2), 199-203.
[21] Degirmenbasi N., Peralta-Inga Z., Olgun U., Gocmez H., Kalyon D.M., Recrystallization of CL-20 and HNFX from Solution for Rigorous Control of the Polymorph Type: Part II, Experimental Studies, *J. Energ. Mater.*, **2006**, *24*(2), 103-139.

[22] Shi X.F., Wang J.Y., Li X.D., An C.W., Preparation and Properties of HMX/Nitrocellulose Nanocomposites, *J. Propul. Power*, **2015**, *31*(2), 757-761.
[23] Kissinger H.E., Reaction Kinetics in Differential Thermal Analysis, *Anal. Chem.*, **1957**, *29*(11), 1702-1706.
[24] Armstrong R.W., Dislocation-Assisted Initiation of Energetic Materials, *Cent. Eur. J. Energ. Mater.*, **2005**, *2*(3), 21-37.
[25] *Vacuum Stability Test − Method Pressure Transducer* (in Chinese), Republic of China National Military Standard, National Defense Science, Technology and Industry Committee, Beijing, **1997**.